

Control of Inclusions in 49MnVS3 Non-Quenched and Tempered Steel by Mg Treatment

Beibei Liu, Hao Zhang, Liangmei Zhong, Yi Wang, Jianxun Fu*

Center for Advanced Solidification Technology (CAST), School of Materials Science and Engineering, Shanghai University, Shanghai, China

Email: *fujianxun@shu.edu.cn

How to cite this paper: Liu, B.B., Zhang, H., Zhong, L.M., Wang, Y. and Fu, J.X. (2022) Control of Inclusions in 49MnVS3 Non-Quenched and Tempered Steel by Mg Treatment. *Journal of Materials Science and Chemical Engineering*, 10, 47-54.
<https://doi.org/10.4236/msce.2022.107004>

Received: January 4, 2022

Accepted: July 26, 2022

Published: July 29, 2022

Abstract

To explore the effect of different Mg contents on the morphology, composition, distribution, and deformation of sulfides in 49MnVS3 non-quenched and tempered steel, the inclusions were observed and counted by Zeiss metallographic microscope and scanning electron microscope, and the inclusions in the compressed samples were compared by Gleeble-3500 thermal simulation test machine. Results showed that the size of sulfide in steel decreases and the distribution uniformity of sulfide are significantly improved with the increase of Mg content. The proportion of composite inclusions in steel increases obviously, and the proportion of individual MnS decreases. The composition of the included core is in accordance with the principle of $Al_2O_3 \rightarrow Al_2O_3 + MgO \cdot Al_2O_3 \rightarrow MgO \cdot Al_2O_3 + MgO \rightarrow MgO \rightarrow MgO + MgS$. After Gleeble compression, the aspect ratio of sulfide inclusions decreases, and the spindle ratio h increases significantly.

Keywords

Mg Treatment, Non-Quenched and Tempered Steel, Sulfide, Composite Inclusions, Gleeble

1. Introduction

49MnVS3 steel, a kind of non-quenched and tempered steel, is widely used in the manufacture of automobile engine connecting rods, crankshafts, and other shaft parts. Since shaft parts need to withstand greater bending stress and impact load, non-quenched and tempered steels are required to possess excellent strength, toughness, fatigue life, and cutting performance [1] [2]. Therefore, controlling

the size, shape, number, and distribution of inclusions in non-quenched and tempered steel is particularly important for improving the mechanical properties of steel. Presently, it is a common “oxide metallurgy” method to modify inclusions in steel by magnesium treatment [3]-[10]. Magnesium reacts with Al_2O_3 inclusions to generate magnesia-aluminum spinel with a smaller size, and the spinel can act as a heterogeneous core particle to induce precipitation of MnS inclusions, which is beneficial to enhance the deformation resistance of MnS [11].

This work aims to describe the evolutions of the oxide-sulfide inclusions in 49MnVS3 steel after the smelting and hot-processing with various masses of Mg addition to steel. Firstly, by adding different mass fractions of magnesium to 49MnVS3 steel, the influence of different magnesium content on the morphology, distribution, composition, quantity, and size of the inclusions was discussed. Secondly, the hot rolling process simulation was carried out by the Gleeble-3500 thermal simulation test machine, and the deformation of the sulfide in the actual rolling process after the magnesium modification treatment was explored.

2. Experimental

2.1. Materials

The raw materials include 49MnVS3 steel casting billet as well as Ni-Mg alloy (75%:25%), quartz tubes, molybdenum rods, and high purity Ar gas (99.999%). The chemical composition of the sample is shown in **Table 1**.

2.2. Methods

A total of five groups of magnesium treatment modification experiments were conducted, which were divided into one contrast group and four experimental groups with different quality magnesium alloys. The experimental procedures were as follows: 600 g of original billet steel was placed into a magnesia crucible (ID: 53 mm, OD: 61 mm, H: 120 mm), and transferred into a pit-type resistance furnace. Then, the sample was heated to 1873 K under high-purity argon flow (15 L/min), and the molten steel was held for 20 min to achieve sufficient homogenization.

The final content of magnesium of the melts is listed in **Table 2**.

After the experiment, the metallographic samples of 10 mm × 10 mm × 12 mm were obtained at the 1/4 diameter of the center of the ingot. The samples were polished and observed under optical microscope (Zeiss) and scanning electron microscope (SEM, Model: Phenom Pro) to observe the morphology of the inclusions.

Table 1. The chemical composition of 49MnVS3 steels (wt%).

C	Si	Mn	P	S	Al _t
0.47	0.35	0.92	0.013	0.047	0.012

Table 2. Measurements results of magnesium and yield.

Code	Ni-Mg alloy (g)	Mg (wt%)	Ca (wt%)	Yield (wt%)
1	0	-	0.0006	-
2	0.58	0.0007	0.0006	3.75
3	0.80	0.0010	0.0006	3.16
4	1.06	0.0019	0.0006	3.37
5	2.01	0.0022	0.0006	2.10

3. Results and Discussion

3.1. Effect of Mg Content on the Morphology and Quantity of Inclusions

Define abbreviations and acronyms the first time they are used in the text, even after they have been defined in the abstract. Abbreviations such as IEEE, SI, MKS, CGS, sc, dc, and rms do not have to be defined. Do not use abbreviations in the title or heads unless they are unavoidable.

The morphology and distribution of inclusions in the sample were observed by metallographic microscope, and the typical distribution of the five groups of inclusions was shown in **Figure 1**. As shown in **Figure 1(a)**, when only Ca is added to the non-quenched and tempered steel, inclusions are irregularly distributed, and inclusions are aggregated and distributed in the grain boundary in the form of long chains. In addition, there are many inclusions in large size and few in small size. After adding Mg and Ca for composite treatment, it can be seen from **Figures 1(b)-(e)** that the distribution of inclusions becomes more uniform and the morphology of inclusions transforms from chain shape to spherical or spindle shape, while the large particle inclusions are significantly reduced.

3.2. Effect of Mg Content on the Composition of Inclusions

In order to explore the detailed changes of the inclusions in the steel during the composite treatment of different mass fractions of magnesium, the morphology and composition of the inclusions in the sample were analyzed by SEM with energy spectrometer, as shown in **Figure 2**.

According to **Figure 2**, magnesium can simultaneously modify oxides and sulfides to form oxide-sulfide composite inclusions. The mechanism of Mg modification is analyzed: Magnesium bubbles have a strong binding ability with dissolved oxygen in molten steel. When Mg is added into molten steel, it will preferentially react with Al and O to form $\text{MgO}\cdot\text{Al}_2\text{O}_3$. If the mass fraction of magnesium continues to increase, $\text{MgO}\cdot\text{Al}_2\text{O}_3$ will further react with Mg to form MgO. In addition, a very small amount of magnesium reacts with sulfur to form MgS. At the end of solidification, $\text{MgO}\cdot\text{Al}_2\text{O}_3$, MgO and a tiny amount of MgS induce the encapsulation of sulfide to form composite inclusions.

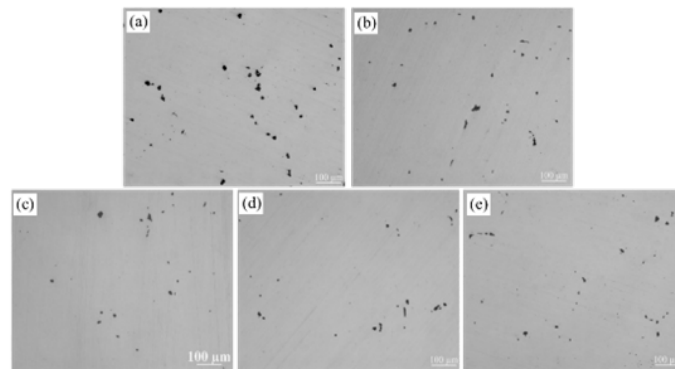


Figure 1. Optical morphologies of the inclusions with various Mg additions. (a) 0 ppm; (b) 7 ppm; (c) 10 ppm; (d) 19 ppm; (e) 22 ppm.

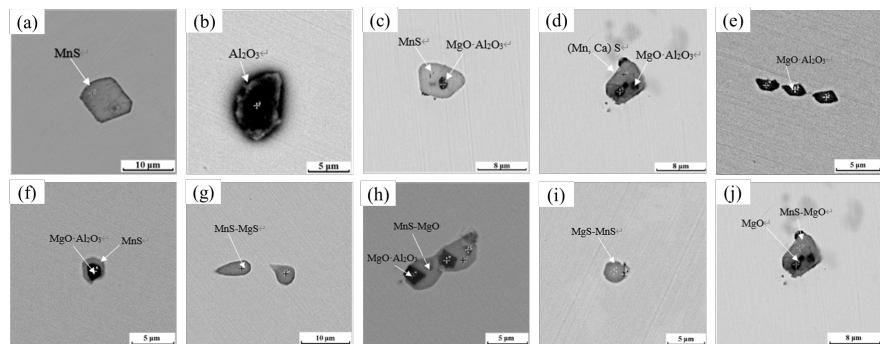


Figure 2. Compositions of inclusion after Mg addition. (a), (b) 0 ppm; (c), (d) 7 ppm; (e), (f) 10 ppm; (g), (h) 19 ppm; (i), (j) 22 ppm.

The change of the oxide core in the composite sulfides with the increase of magnesium content is: $\text{Al}_2\text{O}_3 \rightarrow \text{Al}_2\text{O}_3 + \text{MgO} \cdot \text{Al}_2\text{O}_3 \rightarrow \text{MgO} \cdot \text{Al}_2\text{O}_3 + \text{MgO} \rightarrow \text{MgO} \rightarrow \text{MgO} + \text{MgS}$. The Mg in the composite sulfide (Mg, Mn)S wrapping around the Mg-Al-O oxide core is mainly derived from the diffusion of Mg in the oxide core into the outer MnS.

The ratio of composite sulfide and the ratio of individual MnS with different magnesium content are obtained, as shown in **Table 3**. The content of composite sulfide with core corresponding to magnesium addition of 0 ppm, 7 ppm, 10 ppm, 19 ppm, 22 ppm are 6.7%, 13.7%, 40.2%, 44.6%, 50.5%, and the percentages of individual MnS are 93%, 83%, 57.8%, 53.4%, 47.5%, respectively.

3.3. Effect of Mg Content on the Deformability of Inclusions

In order to explore the deformation mechanism of the inclusions after magnesium treatment in the actual rolling process, this experiment used the Gleeble-3500 thermal simulation tester to simulate the hot rolling process. The simulated rolling material is the half of the ingot in the high-temperature furnace modification experiment. The deformation temperature, deformation speed and degree of deformation of the sample can be accurately controlled on the thermal simulation testing machine. It can also deform the sample in multiple passes. After deformation, it can control the cooling of the sample. Some steel samples (diameter

Table 3. Quantitative statistics of the content of composite inclusions and MnS.

Mg (ppm)	Compound inclusion (%)	MnS (%)
0	6.7	93
7	13.7	83
10	40.2	57.8
19	44.6	53.4
22	50.5	47.5

of 10 mm and height of 15 mm) were used to conduct single-direction compression rolled experiments.

The process of this experiment is as follows. First, the rolled sample was heated to a rolling temperature of 1200°C at 5°C·s⁻¹, and then the temperature was maintained for 5 minutes. Next, as shown in **Figure 3**, the sample was rolled by gleeble-3500, the total deformation along the horizontal axis was 60%, and the rolling time was 0.1 s. After rolling, the rolled sample is cooled by air, and then polished and imaged. The metallographic image is shown in **Figure 4**.

It can be seen from **Figure 4** that the sulfide in the original 49MnVS3 steel is still in a long strip shape after the simulated compression. After modification by adding Mg, the morphology of the sulfide varied from a long strip to a short rod or spindle shape. The result shows that as the magnesium content increases, the degree of deformation of MnS decreases. This is due to the effect of Mg modification treatment, the proportion of single MnS in the steel decreases and the proportion of composite inclusions with core increases. Some studies [12] [13] [14] have shown that composite inclusions have the characteristics of soft outside and hard inside. Compared with MnS with good plasticity, such inclusions are not easy to deform along the rolling direction during hot working, which can significantly improve the mechanical properties of steel and eliminate anisotropy.

A statistical software is used to perform statistics on metallographic photos to explore the degree of deformation of MnS. For each sample, count the inclusions in 100 metallographic photos. According to the observation results of the metallographic microscope, the shape of inclusions is defined as length/width (L/W), which can be divided into three types: spherical, spindle, long strip and irregular shape. In order to quantitatively describe the deformability of inclusions, the spindle ratio h of the morphology of the inclusions is defined. The spindle ratio h of the inclusions is calculated according to Equation (1), as follows:

$$h = \frac{\text{Spherical number} + \text{Spindle number}}{\text{Total inclusion number}} \quad (1)$$

After the rolling, the L/W values are recorded as shown in **Figure 5**.

Figure 5 shows the h -value ($1 \leq L/W \leq 3$) of sulfide inclusion in non-quenched and tempered steel before and after Mg-Ca composite modification. After Gleeble extrusion of the Mg-added sample in the laboratory, the inclusion spindle rate h

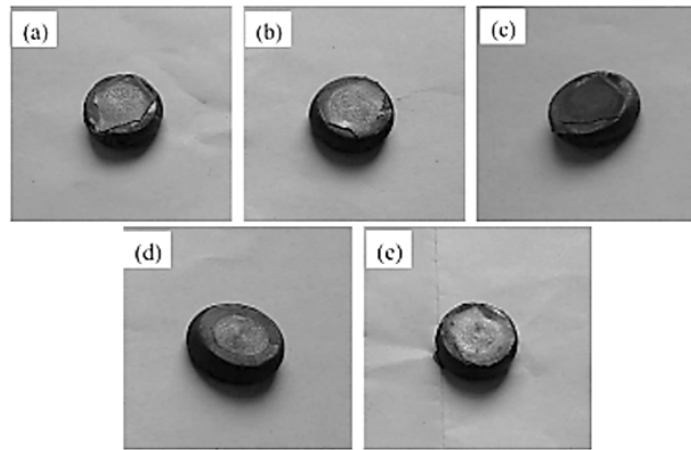


Figure 3. Sample treated with Gleeble. (a) 0 ppm; (b) 7 ppm; (c) 10 ppm; (d) 19 ppm; (e) 22 ppm.

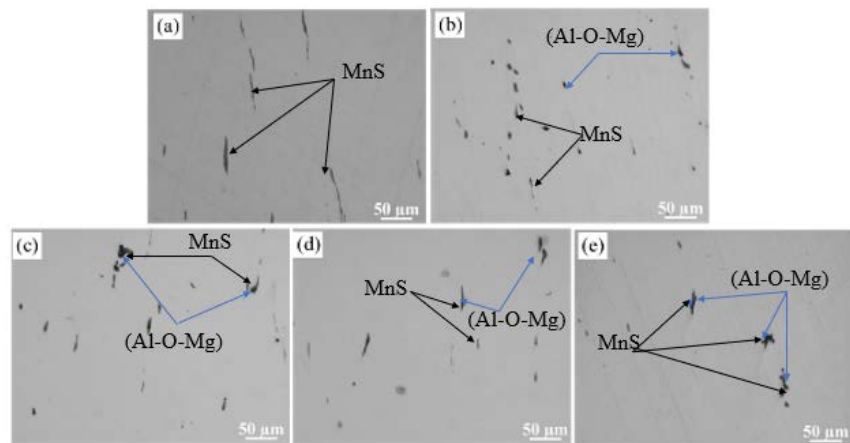


Figure 4. Morphology of sulfide after hot rolling simulation experiment. (a) 0 ppm; (b) 7 ppm; (c) 10 ppm; (d) 19 ppm; (e) 20 ppm.

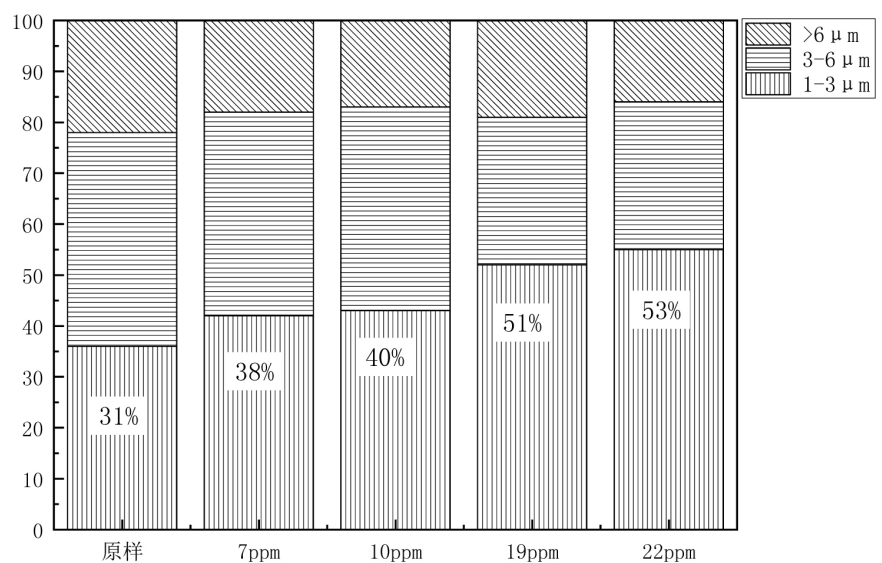


Figure 5. L/W ratio versus various Mg additions after rolling.

increases compared to the original steel with only calcium. When the Mg content in steel changed from 0 to 22 ppm, the spindle rate h of inclusions in steel increased from 31% to 53%. Combined with **Table 3**, it can be seen that this is because the inclusion core rate of sample e is 50.5%, which is significantly higher than that of sample (a) of 6.7%. The greater the h -value, the number of nucleation cores of composite sulfides. However, numerous composite sulfides with oxide cores could contribute to the small deformation of inclusions during hot-processing and further improve the machinability of steel. Therefore, the Mg addition of 10 to 22 ppm in this non-quenched and tempered steel is beneficial to obtaining more spindle inclusions. Simultaneously, the ratio of composite inclusions with cores can be reaching about 40% - 50%.

4. Conclusions

The main conclusions can be summarized as follows:

1) After adding magnesium to the non-quenched and tempered steel, the size of sulfide in steel decreases and the distribution uniformity of sulfide are significantly improved. The proportion of composite inclusions in steel increases significantly, and the proportion of individual MnS decreases.

2) With the increase of magnesium content, the composition of the included core is transformed according to $\text{Al}_2\text{O}_3 \rightarrow \text{Al}_2\text{O}_3 + \text{MgO} \cdot \text{Al}_2\text{O}_3 \rightarrow \text{MgO} \cdot \text{Al}_2\text{O}_3 + \text{MgO} \rightarrow \text{MgO} \rightarrow \text{MgO} + \text{MgS}$. The Mg in the composite sulfide (Mg, Mn)S wrapping around the Mg-Al-O oxide core is mainly derived from the diffusion of Mg in the oxide core into the outer MnS.

3) After Gleeble compression of the magnesium-added samples in the laboratory, the spindle rate h of sulfide increased significantly. This kind of composite sulfide with the core is not easy to extend and deform during hot working, which makes the machinability of steel better, and the reduction of transverse mechanical properties is improved. In the actual production process of non-quenched and tempered steel, when the content of Mg is 10 to 22 ppm, more spindle-like sulfide inclusions can be obtained.

Acknowledgements

The authors gratefully express their appreciation to the National Natural Science Foundation of China (Grant No. 52074179 and 51874195).

Conflicts of Interest

The authors declare no conflicts of interest regarding the publication of this paper.

References

- [1] Davim, J.P., Gaitonde, V.N. and Karnik, S.R. (2008) Investigations into the Effect of Cutting Conditions on Surface Roughness in Turning of Free Machining Steel by ANN Models, *Journal of Materials Processing Technology*, **205**, 16-23.
<https://doi.org/10.1016/j.jmatprotec.2007.11.082>

- [2] Cerullo, M. (2014) Sub-Surface Fatigue Crack Growth at Alumina Inclusions in AISI 52100 Roller Bearings. *Procedia Engineering*, **74**, 333-338. <https://doi.org/10.1016/j.proeng.2014.06.274>
- [3] Zhang, T.S., Wang, D.Y. and Liu, C.W. (2014) Modification of Inclusions in Liquid Iron by Mg Treatment. *Journal of Iron and Steel Research, International*, **21**, 99-103. [https://doi.org/10.1016/S1006-706X\(14\)60130-8](https://doi.org/10.1016/S1006-706X(14)60130-8)
- [4] Shen, P. and Fu, J. (2019) Morphology Study on Inclusion Modifications Using Mg-Ca Treatment in Resulfurized Special Steel. *Materials (Basel, Switzerland)*, **12**, Article 197. <https://doi.org/10.3390/ma12020197>
- [5] Liu, Y. and Zong, N. (2017) Effects of Al-Mg Alloy Treatment on Behavior and Size of Inclusions in SUH 409L Stainless Steel. *Metallurgical Research & Technology*, **115**, Article No. 111. <https://doi.org/10.1051/metal/2017085>
- [6] Fu, J., Yu, Y.G., Wang, A.R. and Chen, B.P. (2009) Inclusion Modification with Mg Treatment for 35CrNi3MoV Steel. *Journal of Materials Science & Technology*, **14**, 53-56.
- [7] Xie, J.B., Zhang, D. and Yang, Q.K. (2018) Exploration of Morphology Evolution of the Inclusions in Mg-Treated 16MnCrS5 Steel. *Ironmaking & Steelmaking*, **46**, 564-573. <https://doi.org/10.1080/03019233.2018.1492501>
- [8] Xu, J., Yang, Q.K. and Cheng, J. (2017) The Evolution and Thermodynamic Analysis of Inclusions in Gear Steel after Magnesium Treatment. *Proceedings of the 2017 International Conference on Manufacturing Engineering and Intelligent Materials (ICMEIM)*, Advances in Engineering, Vol. 100, 511-515. <https://doi.org/10.2991/icmeim-17.2017.86>
- [9] Sun, H., Wu, L.P. and Xie, J.B. (2020) Inclusions Modification and Improvement of Machinability in a Non-Quenched and Tempered Steel with Mg Treatment. *Metallurgical Research & Technology*, **117**, Article No. 208. <https://doi.org/10.1051/metal/2020021>
- [10] Lin, S.G., Yang, H.H. and Su, Y.H. (2019) CALPHAD-Assisted Morphology Control of Manganese Sulfide Inclusions in Free-Cutting Steels. *Journal of Alloys and Compounds*, **779**, 844-855. <https://doi.org/10.1016/j.jallcom.2018.11.290>
- [11] Yang, S., Wang, Q. and Zhang, L. (2012) Formation and Modification of MgO-Al₂O₃-Based Inclusions in Alloy Steels. *Metallurgical and Materials Transactions B*, **43**, 731-750. <https://doi.org/10.1007/s11663-012-9663-1>
- [12] Zhang, T., Liu, C. and Mu, H. (2018) Inclusion Evolution after Calcium Addition in Al-Killed Steel with Different Sulphur Content. *Ironmaking & Steelmaking*, **45**, 447-456. <https://doi.org/10.1080/03019233.2017.1284420>
- [13] Wang, L., Yang, S. and Li, J. (2017) Effect of Mg Addition on the Refinement and Homogenized Distribution of Inclusions in Steel with Different Al Contents. *Metallurgical and Materials Transactions B*, **48**, 805-818. <https://doi.org/10.1007/s11663-017-0915-y>
- [14] Ma, W., Bao, Y. and Wang, M. (2014) Effect of Mg and Ca Treatment on Behavior and Particle Size of Inclusions in Bearing Steels. *ISIJ International*, **54**, 536-542. <https://doi.org/10.2355/isijinternational.54.536>